

# Dalton Transactions

An international journal of inorganic chemistry

Accepted Manuscript

This article can be cited before page numbers have been issued, to do this please use: Q. Zhang, J. Shu, Y. Zhang, Z. Xu, J. Yue, X. Liu, B. Xu, Z. Chen and W. Jiang, *Dalton Trans.*, 2020, DOI: 10.1039/D0DT01823F.



This is an Accepted Manuscript, which has been through the Royal Society of Chemistry peer review process and has been accepted for publication.

Accepted Manuscripts are published online shortly after acceptance, before technical editing, formatting and proof reading. Using this free service, authors can make their results available to the community, in citable form, before we publish the edited article. We will replace this Accepted Manuscript with the edited and formatted Advance Article as soon as it is available.

You can find more information about Accepted Manuscripts in the [Information for Authors](#).

Please note that technical editing may introduce minor changes to the text and/or graphics, which may alter content. The journal's standard [Terms & Conditions](#) and the [Ethical guidelines](#) still apply. In no event shall the Royal Society of Chemistry be held responsible for any errors or omissions in this Accepted Manuscript or any consequences arising from the use of any information it contains.

## ARTICLE

## Structures and Esterolytic Reactivity of Novel Binuclear Copper(II) Complexes with Reduced L-Serine Schiff Bases as Mimic Carboxylesterases

Received 00th January 20xx,  
Accepted 00th January 20xx

DOI: 10.1039/x0xx00000x

Qin Zhang,<sup>a</sup> Jun Shu,<sup>a</sup> Yajun Zhang,<sup>b</sup> Zhigang Xu,<sup>b</sup> Jian Yue,<sup>a</sup> Xiaoqiang Liu,<sup>\*\*a</sup> Bin Xu,<sup>a</sup> Zhongzhu Chen<sup>b</sup> and Weidong Jiang<sup>\*a</sup>

Three novel binuclear copper (II) complexes with reduced L-serine Schiff bases were synthesized, and their structures were analyzed with single crystal X-ray diffraction and DFT calculation. Crystal data reveal all of these binuclear complexes are chiral. Both of 5-halogenated (bromo- and chloro-) binuclear complexes exhibit right-hand helix structural character. Interestingly, 5-methyl-containing analogue constructs a two-dimensional pore structure. In this paper, esterolysis reactivity of the as-prepared complexes show that in the hydrolysis of p-nitrophenyl acetate (PNPA) these three complexes provide 26, 18, 40-fold rate acceleration as compared to spontaneous hydrolysis of PNPA at pH 7.0, respectively. Under selected conditions, in buffered aqueous solution excess three orders of magnitude rate enhancement were observed for the catalytic hydrolysis of another carboxylic ester, p-nitrophenyl picolinate (PNPP). Furthermore, these complexes efficiently promote the PNPP hydrolysis in a micellar solution of cetyltrimethylammonium bromide (CTAB), giving rise to excess four orders of magnitude rate enhancement which is approximate 2.0~3.2 times higher than that in buffer.

### Introduction

Carboxylesterases (CEs) as B-type esterolases play vital role in some physiological activity,<sup>1</sup> thereby maintaining the normal physiological function of the body. In addition, natural esterases display high activity and selectivity due to multiple molecular activation and specific substrate binding.<sup>2</sup> Owing to intrinsic environmental sensitivity of natural CEs, it was highly limited that the expansion of the application of CEs from the physiological activities to other fields. To overcome the above defects, most of scientists devoted to develop various artificial esterases and evaluated their activities

towards different substrates including esters,<sup>3</sup> amides<sup>4</sup> and plasmid DNA.<sup>5</sup> In general, chemists are eagerly anticipant of the successful construction of the active centers in which includes three essential domains (e.g., the binding site, catalytic site and hydrophobic cave)<sup>6</sup> that should be regarded to be typical structural characters of enzymes.

As for natural metallohydrolases, central metal ions in active domain play vital role in catalytic hydrolysis reactions.<sup>7</sup> That is, at least four key roles should be considered for central metal<sup>8</sup>: (1) activating substrate; (2) activating nucleophilic reagent; (3) activating leaving group; (4) stabilizing negative tetrahedron transition state (TS). Along this line of consideration, a great deal of metal complexes as enzyme models were designed to simulate those features of natural CEs.<sup>9</sup> As we know, Schiff bases metal complexes with features of convenient synthesis and structural modification were widely applied in the fields of biological applications,<sup>10</sup> functional materials<sup>11</sup> and artificial metalloenzyme.<sup>12</sup> Among these applications mentioned above, Schiff bases metal complexes were widely selected as mimic hydrolases<sup>13</sup> to hydrolytically cleave the varied esters, proteins and DNA. And, further elucidations involve in the effects of various structural modulation strategies (steric hindrance, electronic effect, rigid-flexible adjustment, etc) on hydrolytic reactivity.

Owing to good biocompatibility of amino acid Schiff bases and corresponding metal complexes, and thereby studying their design and functions has become a hot pot. At present, some amino acid Schiff base complexes have been evaluated their activities for the hydrolysis of esters<sup>14</sup> besides their biological activity.<sup>15</sup> Generally,

<sup>a</sup> School of Chemistry and Environmental Engineering, Sichuan University of Science & Engineering, Sichuan Zigong 643000, P. R. China

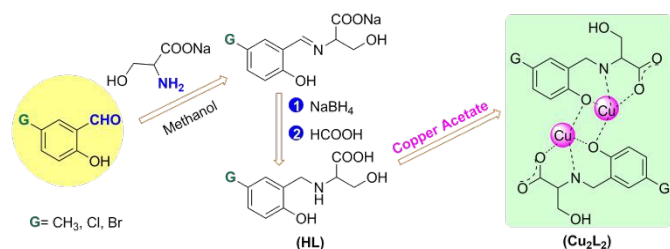
E-mail: jwdx@use.edu.cn; xqliu@use.edu.cn

<sup>b</sup> College of Pharmacy, National & Local Joint Engineering Research Center of Targeted and Innovative Therapeutics, Chongqing Key Laboratory of Kinase Modulators as Innovative Medicine, Chongqing University of Arts and Sciences, Chongqing 402160, China.

Electronic Supplementary Information (ESI) available: crystal structures of the two reduced L-serine Schiff bases and three copper(II) complexes, molecule structures and topological structures of binuclear copper(II) complexes, representations of the charge density difference, HOMO and LUMO orbitals for two halogenated complexes, thermal analysis and electronic spectra of three binuclear copper(II) complexes used in this work, representative UV-vis absorbance scan for the hydrolysis of PNPA and PNPP by Cu<sub>2</sub>L<sub>2</sub>, ESI-MS spectra for the Cu<sub>2</sub>L<sub>2</sub>-promoted hydrolysis of PNPP or PNPA, Crystal parameters of binuclear copper(II) complexes with reduced Schiff bases, selected bond lengthen(Å) and angle (deg) of binuclear copper(II) complexes, Calculated Addison Tau factors (τ) and geometry for the central copper(II) of binuclear copper(II) complexes, DFT-calculated Mulliken charges of the two central copper(II) ions of each complexes used here, relative activities of PNPP hydrolysis between various catalytic systems. Crystallographic Information Files (CIF) were also provided.

See DOI: 10.1039/x0xx00000x

appropriate rigid-flexibility of the active site is required for native enzymes to which the substrate could be bound as described in 'Induce-Fit Hypothesis' by D. E. Koshland<sup>16</sup> and the developed theory by C. L. Tsou.<sup>17</sup> Though those mimic metallohydrolases with amino acid Schiff bases exhibited good activities for esterolysis, their rigid structures probably limit the binding of substrate on the central metal during the substrate hydrolysis. Taking account into this reason, herein we decided to synthesize three reduced L-Serine Schiff bases and their copper (II) complexes with more flexible frame (Scheme 1). Furthermore, catalytic activities of the as-prepared complexes as potential artificial metallohydrolases were evaluated for the hydrolysis of p-nitrophenyl acetate (PNPA). In order to investigate different substrate selectivity, a similar substrate (p-nitrophenyl picolinate, PNPP) was used as reference for evaluating the different selectivity of these complexes under comparable conditions. With regard to native enzymes, additionally, catalytically active site and substrate binding domain generally exist inside hydrophobic pocket of enzymes.<sup>18</sup> This hydrophobic domain is essential to high activity and selectivity of natural enzymes. To simulate this feature of enzymes, many researchers have constructed hydrophobic microenvironment of some artificial esterolase models mainly including metallosurfactants<sup>19</sup> or mixed systems of metal complexes and various micelles.<sup>20</sup> Hence, in the present work we are intrigued to study a selected micellar effect of cationic cetyltrimethylammonium bromide (CTAB) on the PNPP hydrolysis promoted by the as-synthesized binuclear copper(II) complexes with reduce L-Serine Schiff bases.



**Scheme 1.** Synthesis route of binuclear copper (II) complexes with reduced L-Serine Schiff Bases.

## Results and Discussion

### 2.1 Structures Analysis of Binuclear Copper Complexes with Reduced L-Serine Schiff Bases

In the present work, three binuclear copper(II) complexes were successfully synthesized with a coordination reaction of the as-synthesized reduced L-serine Schiff bases and cupric acetate monohydrate. Scheme 1 shows the synthesis route of desired binuclear copper(II) complexes. Single crystals of these complexes were successfully collected and further be structural analysed. Figure 1 depicts the asymmetrical units of three binuclear copper(II) complexes on the basis of original crystal data shown in Figure S-1. Corresponding molecule structures and 2D network structures were given in Figure S-2. Collected crystal data and selected bond parameters of three complexes were shown in Tables S-1 and S-2, respectively.

Molecule structures in Figure S-2 reveal that each binuclear copper(II) complex used is phenoxo-bridged dicopper(II) one with

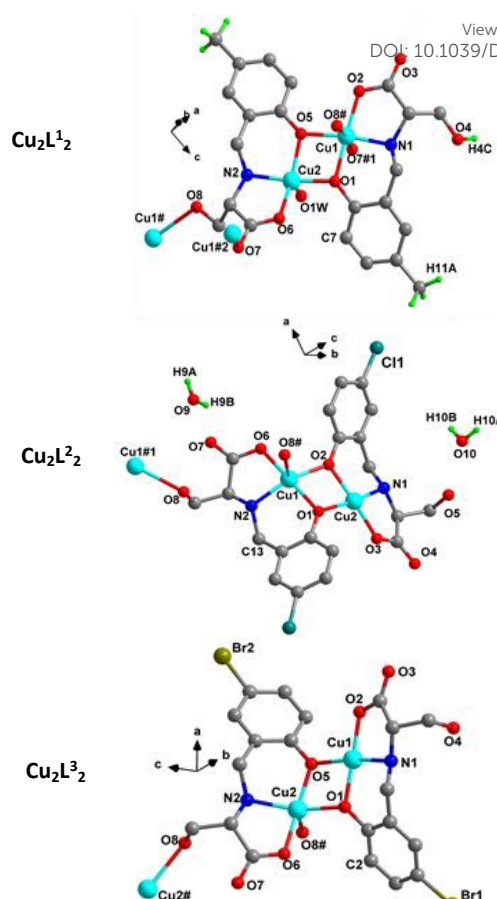


**Figure 1.** Asymmetrical units of the as-synthesized binuclear copper(II) complexes with reduced L-serine Schiff bases.

'ONO' tridentate ligand. Different geometries for these complexes are obtained. The crystal of Cu<sub>2</sub>L<sub>1</sub><sup>2</sup> (CCDC No. 2004683) containing 5-methyl group is orthorhombic with unit-cell parameters: a=7.527, b=14.125, and c=23.965 Å; space group P2<sub>1</sub>2<sub>1</sub>2<sub>1</sub>/c; Z=4. Four complex molecules are distributed in each crystal cell of Cu<sub>2</sub>L<sub>1</sub><sup>2</sup>, and the other two complexes display monoclinic crystal system with P2<sub>1</sub>/c space group with each crystal cell including two complex molecules (left column of Figure 2). As for Cu<sub>2</sub>L<sub>1</sub><sup>2</sup>, an asymmetric coordination sphere was assigned to their two copper centers. Penta-coordinated structure of the Cu(2) cation with slightly distorted rectangular-pyramidal configuration with Addison Tau factor<sup>21</sup> (τ=0.26) was appeared as accompanying with the binding of one water molecule. The slightly distorted octahedral configuration feature (τ=0.08) was assigned to the hexacoordinate Cu(1) cation of Cu<sub>2</sub>L<sub>1</sub><sup>2</sup>. Interestingly, the 2D staggered network structure (the right graph of Figure S-2A) of forming a smaller cavity (marked with broken orange-yellow circle) was constructed via the Cu(1) coordination site filled by intermolecular interactions with alkoxo oxygen (O7#1) and one carboxylic oxygen (O8#) of L-serine. In terms of two halogenated complexes (Cu<sub>2</sub>L<sub>2</sub><sup>2</sup>: CCDC No. 2004684, Cu<sub>2</sub>L<sub>3</sub><sup>2</sup>: CCDC No. 2004685), one can observe the almost same characteristics for the molecular structure and crystal packing shown in Figures S-2B and 2C. Namely, the one Cu(II) ion of them has a slightly distorted tetrahedral configuration and the other one is square planar, which is confirmed by τ factors shown in Table S-3. Intriguingly, 1D periodic right-hand

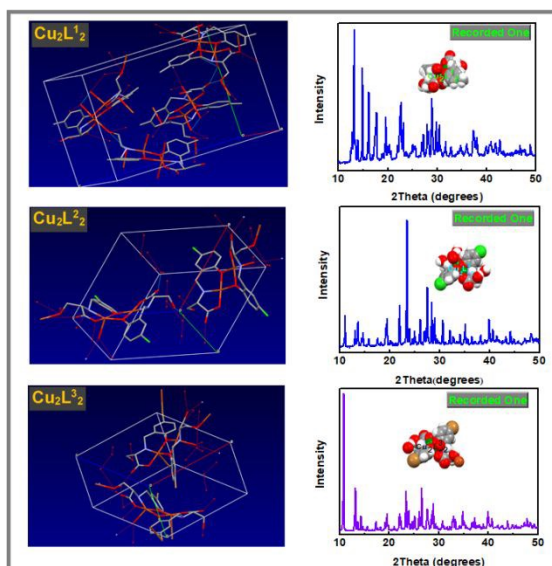


**Figure 2.** Crystal cells (left column) and recorded PXRD (right column) of three binuclear copper(II) complexes.

helix structure and 2D supramolecular network texture were originated from  $\pi$ - $\pi^*$  stacking with approximate 4.0 Å spacing between two benzene rings respectively located in neighboring 1D helix structures. The Cu-Cu distance of each binuclear Cu(II) complex is about 3.0 Å that is match with the favourable metal-metal distance of most of natural enzymes.<sup>22</sup> As shown in the right column of Figure 2, recorded PXRD patterns were given for three binuclear copper(II) complexes. A serial of sharp peaks in a  $2\theta$  range of 10° to 50° suggest a high degree of crystallization for each binuclear copper(II) complex used here.

In this work, all the density functional theory (DFT) calculations were carried out by DMol3 code. The generalized gradient approximation (GGA) with Perdew-Burke-Ernzerhof (PBE) functional was used to describe the exchange and correlation functionals. In order to accurately describe noncovalent forces, Grimme is applied to dispersion correction for DFT. For more detailed parameters setting of simulation, see the previous work of Liu et al.<sup>23</sup> Both the charge density difference and the molecular orbital interactions are respectively illustrated in Figure 3 (for  $\text{Cu}_2\text{L}^1_2$ ) and Figure S-3 (for  $\text{Cu}_2\text{L}^2_2$  and  $\text{Cu}_2\text{L}^3_2$ ), blue area indicates electron accumulation, whereas the yellow region shows the electron depleted. Judging from the charge density difference, copper atoms in binuclear copper(II) complexes are electron-deficient, and corresponding Mulliken charges (Table S-4) are predicted to be 0.569 ~ 0.573 e for  $\text{Cu}_2\text{L}^1_2$ , 0.576 ~ 0.586 e for  $\text{Cu}_2\text{L}^2_2$  and 0.580 ~ 0.581 e for  $\text{Cu}_2\text{L}^3_2$ . To obtain a more detailed qualitative description of the binuclear copper(II) complexes with reduced L-serine Schiff bases, the HOMO and LUMO orbitals of them have been calculated. As can be observed in Figure 3, the HOMOs are mainly ligand  $\pi$  orbitals for the centrosymmetric square-planar of binuclear copper(II) complexes, whereas the d orbitals of copper(II) ion have small contribution to orbitals of these complexes. The copper(II) metal centers use  $d_{xy}$  type orbitals, not  $d_{x^2-y^2}$  orbitals, for a  $\sigma^*$  interaction with the p orbitals of N and O atoms.

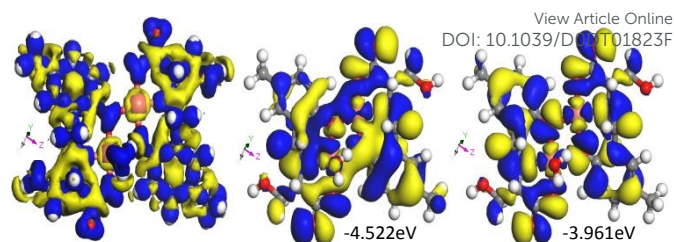


**Figure 3.** Representations of the charge density difference (left column), HOMO (central column) and LUMO (right column) orbitals of  $\text{Cu}_2\text{L}^1_2$ . Those DFT-calculated results for  $\text{Cu}_2\text{L}^2_2$  and  $\text{Cu}_2\text{L}^3_2$  are shown in Figure S-3 for clarity.

In addition, the thermal analysis reveals that all of three complexes possess high thermostability and have no definite melt point (Figure S-4A-C). Thermogravimetric (TG) curves illustrate that these complexes undergo gradually thermal decomposition and lose some small molecules or structural fragments with respective 46.65%, 51.62% and 60.14% of residual mass in the operated temperature range. As shown in differential thermal gravity (DTG) curves, three complexes sharply decompose in the range of 225 °C to 260 °C with respective peak temperature (e.g., 231.89°C for  $\text{Cu}_2\text{L}^1_2$ , 240.36°C for  $\text{Cu}_2\text{L}^2_2$ , 246.42°C for  $\text{Cu}_2\text{L}^3_2$ ). Mass losing of 5.54% shall be assigned to the departure of two crystal waters of  $\text{Cu}_2\text{L}^2_2$  accompanying with an apparent endothermic peak around 100°C shown in DSC analysis. Also, DSC curve of  $\text{Cu}_2\text{L}^3_2$  shows the losing of two crystal waters around 75°C. Combining DSC with TG of  $\text{Cu}_2\text{L}^1_2$ , it was found that there is 3.18% of mass lose but no endothermic signal implying the exist of a small amount of adsorbed water in the  $\text{Cu}_2\text{L}^1_2$  sample. Overall, thermal analysis shows 5-bromo-substituted  $\text{Cu}_2\text{L}^3_2$  possesses the best thermal stability.

The UV-vis electronic spectra of these three complexes were recorded in a wavelength region of 190 to 600nm (Figure S-4D). It was found that each complex has a strong and sharp absorption in the near-UV wavelength range (around 210nm). The electronic spectra show a single absorption band at 209 nm for  $\text{Cu}_2\text{L}^1_2$  and  $\text{Cu}_2\text{L}^2_2$ , and 211 nm for bromo-containing  $\text{Cu}_2\text{L}^3_2$ . The absorptive positions around 210 nm of these bands are typical of  $\pi$ - $\pi^*$  transition of multiply substituted benzene ring. Red shift of 2nm on  $\lambda_{\text{max}}$  and strengthened absorption were observed in characteristic absorption of  $\text{Cu}_2\text{L}^3_2$ . This is probably contributed to a n- $\pi$  conjugation inspiration and hyperchromicity due to the introducing of bromine group as auxochrome group. According to Lambert-Beer law, furthermore, related molar absorption coefficients ( $\epsilon$ ) are determined and listed in Table 1. The  $\epsilon$  values show an increased trend along with the introducing of the 5-substituted groups as following order:  $\text{CH}_3 < \text{Cl} < \text{Br}$ . The biggest absorbance with a value of 2.401 was observed for bromo-containing  $\text{Cu}_2\text{L}^3_2$  compared to  $\text{Cu}_2\text{L}^1_2$  and  $\text{Cu}_2\text{L}^2_2$  at the same sample concentration.

**Table 1** Electronic spectra parameters of three copper(II) complexes at 25°C

| Catalyst                  | $\lambda_{\text{max}}$ (nm) | Abs   | $\epsilon$ ( $\text{L} \cdot \text{mol}^{-1} \cdot \text{cm}^{-1}$ ) | Electronic Transition   |
|---------------------------|-----------------------------|-------|--|-------------------------|
| $\text{Cu}_2\text{L}^1_2$ | 209                         | 1.748 | 26220  | $\pi \rightarrow \pi^*$ |
| $\text{Cu}_2\text{L}^2_2$ | 209                         | 1.976 | 29640  | $\pi \rightarrow \pi^*$ |
| $\text{Cu}_2\text{L}^3_2$ | 211                         | 2.401 | 36015  | $\pi \rightarrow \pi^*$ |

Conditions: 25°C, pH 7.0,  $C_{\text{complex}} = 6.67 \times 10^{-6} \text{ mol L}^{-1}$ .

## 2.2 Hydrolysis Reactivity and Proposed Mechanisms of Binuclear Copper(II) Complexes Towards Carboxylic Esters

In the current work, we mainly focus on the activity of binuclear copper(II) complexes with reduced L-serine Schiff base in the hydrolysis of p-nitrophenyl acetate (PNPA) as classic carboxylic ester model. Besides, another analogue (p-nitrophenyl picolinate, PNPP) was selected as candidate for comparing the possible selectivity of catalyst to the two substrates. Figure S-5A shows the spectral change of the PNPA hydrolysis by  $\text{Cu}_2\text{L}^1_2$  as example in buffered aqueous solution. The absorption strength at 272nm of substrate PNPA gradually decreases along with the extension of reaction time. Moreover, strengthened absorbance at 400nm indicates the increase in concentration of detectable product, p-nitrophenolate anion. The changed trend of UV spectra reveals that the current substrate PNPA is able to be catalytically hydrolysed by  $\text{Cu}_2\text{L}^1_2$ . Similar trend of spectral change (Figure S-5B) was observed for the  $\text{Cu}_2\text{L}^1_2$ -induced hydrolysis of PNPP as a reference substrate.

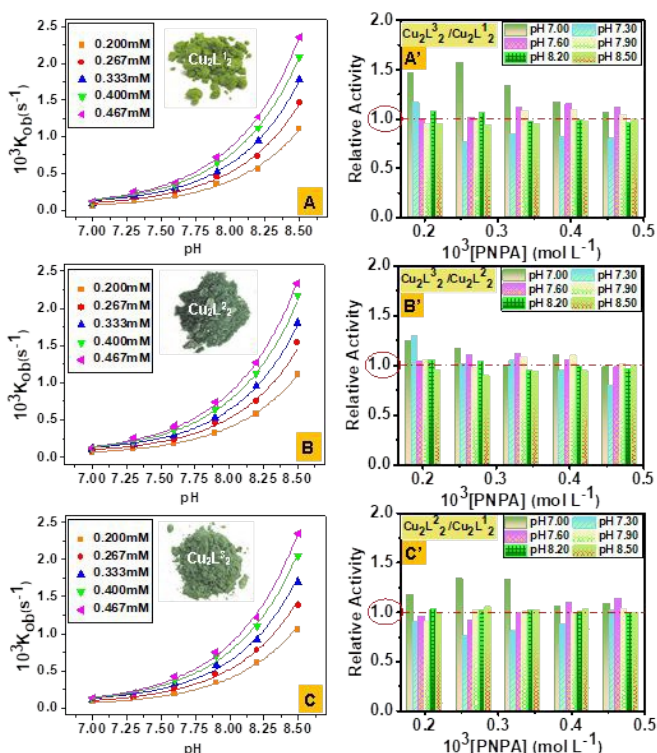


**Figure 4.** Dependence of the hydrolysis rate constants of PNPA upon pH in the presence of as-prepared copper(II) complexes (left, A-B), and relative activity graphs (right, A'-C'). Conditions: 25 °C, I=0.1M KCl,  $C_{\text{complex}}=1 \times 10^{-5} \text{ mol L}^{-1}$ .

In the hydrolytic kinetic determination, the substrate concentration should be more than 20 times of the catalyst concentration. As shown in Figures 4A-C, three copper(II) complexes display gradually increase tendency of  $k_{\text{ob}}$  against pH for the PNPA hydrolysis. Under a comparable condition (pH 7.0, 25 °C, I=0.1 KCl), methyl-substituted  $\text{Cu}_2\text{L}^1_2$  achieves approximately 26-fold rate enhancement in contrast with spontaneous hydrolysis rate<sup>24</sup> of PNPA. Meanwhile, we observed eighteen and forty-fold rate acceleration for 5-chloro- or 5-bromo-substituted complexes ( $\text{Cu}_2\text{L}^2_2$ ,  $\text{Cu}_2\text{L}^3_2$ ). As a whole, in the operated ranges of pH and substrate concentration three 5-substituted groups (-CH<sub>3</sub>, -Cl, -Br) does not

cause significant difference in activity in spite of individual exceptions (Figures 4A'-C'). This result is possibly ascribed to weak electrostatic and steric effects of these substitutes that influencing the activity of these binuclear copper(II) complexes. DFT-calculated Mulliken charges in Table S-4 denote small difference between these three complexes, which also provides evidence for a neglectable impact of Lewis acidity on reactivities of these complexes.

To evaluate the substrate selectivity of the prepared copper complexes, herein we compared hydrolytic behaviour of PNPA with that of PNPP as a contrast substrate (Figure 5) under selected conditions (pH 7.0,  $C_{\text{substrate}}=2.0 \times 10^{-4} \text{ mol L}^{-1}$ ,  $C_{\text{complex}}=1 \times 10^{-5} \text{ mol L}^{-1}$ ). The obtained observations shown in Figure 5A-C reveal that  $\text{Cu}_2\text{L}^1_2$  is relatively much reactive over the other two halogenated complexes,  $\text{Cu}_2\text{L}^2_2$  and  $\text{Cu}_2\text{L}^3_2$ . In non-micellar solution, moreover, all of complexes displayed good reactivity by three orders of magnitude acceleration in comparison with the background rate ( $k_0=7.8 \times 10^{-6} \text{ s}^{-1}$ <sup>25</sup>) of PNPP spontaneous hydrolysis in buffered aqueous solution. Respectively, 6949-, 3862- and 3880-fold rate enhancement was obtained for the PNPP hydrolysis respectively promoted by  $\text{Cu}_2\text{L}^1_2$ ,  $\text{Cu}_2\text{L}^2_2$  and  $\text{Cu}_2\text{L}^3_2$ .

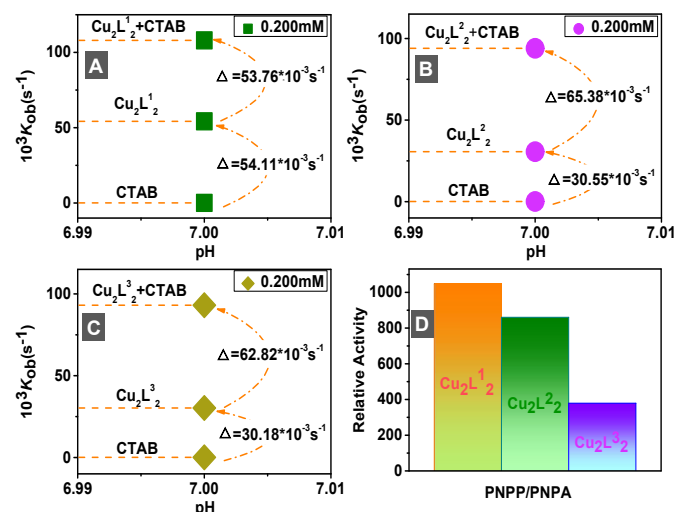


**Figure 5.** Hydrolysis rates (A-C) of PNPP in different catalytic systems. Figure 5D shows the relative activity of PNPP against PNPA. Conditions: pH 7.00, 25.0 °C, [complex]= $1 \times 10^{-5} \text{ mol L}^{-1}$ , [PNPA]= $2.0 \times 10^{-4} \text{ mol L}^{-1}$ , [PNPP]= $2.0 \times 10^{-4} \text{ mol L}^{-1}$ , [CTAB]= $1.0 \times 10^{-3} \text{ mol L}^{-1}$ .

With respect to substrate specificity of natural enzymes, it is mainly contributed to special binding of substrate molecules to binding sites of enzymes surface.<sup>26</sup> According to the hydrolysis process of esters induced by metallohydrolases, the formation of reactive substrate-enzyme binary complex benefits the hydrolysis reaction.<sup>27</sup> In the current work, each complex exhibited distinguishable reactivity towards the hydrolysis of PNPA and PNPP (Figure 5D). The hydrolysis of PNPP is 1047-, 860- and 379-fold faster than that of PNPA. The intrinsic structure of each substrate should be the main cause for the different respond to the selectivity of each catalyst used. With regard to PNPA and PNPP, completely different mechanisms shown in Figure 6 lead to remarkable difference in hydrolysis rate. PNPA hydrolysis undergoes an intermolecular nucleophilic attack of metal-bound OH<sup>-</sup> on the carbonyl of free PNPA

molecule during which no binary catalyst-PNPA complex forms (please refer to ESI-MS spectrum shown in Figure S-6). Conversely, an intramolecular nucleophilic attack was involved in the hydrolysis of PNPP even though no direct ESI-MS evidence (Figure S-6) for the formation of catalyst-PNPP intermediate was temporarily obtained that is probably attributed to highly rapid hydrolysis process of PNPP in the presence of the as-synthesized complexes. As described in previous reports,<sup>28</sup> the intramolecular mechanism for PNPP hydrolysis includes the formation of active PNPP-complex intermediate via a coordination of central Cu(II) ion with pyridine N atom inside PNPP, which possesses a few advantages concerning lower energy barrier and closer substrate-to-nucleophile space against the intermolecular one. Thereupon, PNPP hydrolysis promoted by each binuclear copper(II) complex achieves much obvious rate enhancement compared to PNPA hydrolysis. To some extent this feature provides evidence for the substrate specificity of natural hydrolases,<sup>29</sup> suggesting the artificial enzymes are required favourable substrate structures.

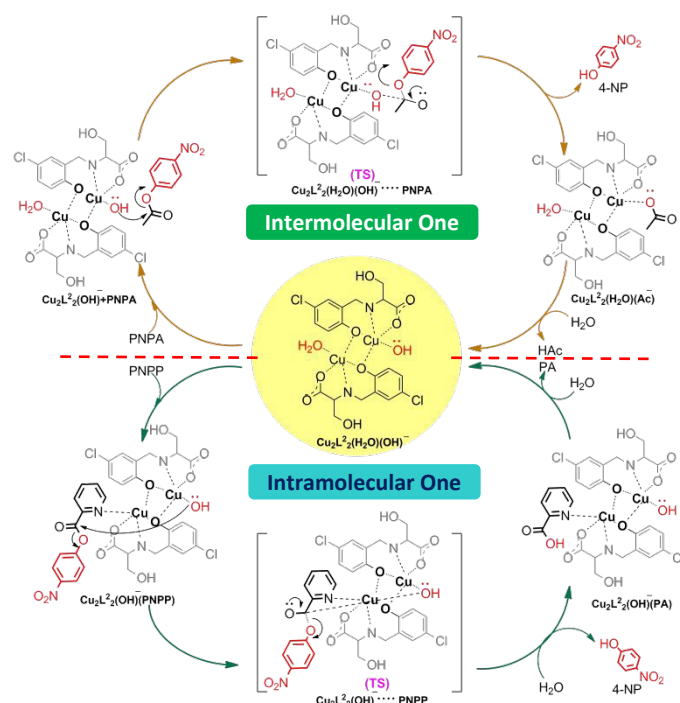
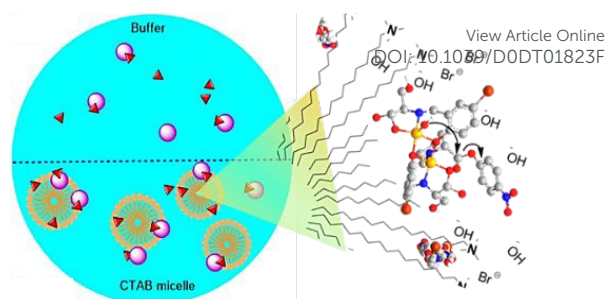


**Figure 6.** Proposed mechanism of PNPA (top) and PNPP (bottom) hydrolysis promoted by  $\text{Cu}_2\text{L}_2$  as an example.

The hydrophobic domain of natural enzyme plays a vital role in catalysis process via hydrophobic and electrostatic interactions.<sup>30</sup> 'Hydrophobic pocket' having low dielectric constants facilitates the insertion of substrate molecules and the facial generation of active nucleophile (e.g.,  $\text{OH}^-$ ).<sup>31</sup> Therefore, in the current work the micellar effect of traditional surfactant CTAB was investigated for evaluating possible positive function of CTAB micelles in the PNPP hydrolysis. As shown in Figure 5A-C, excess four orders of magnitude rate enhancement achieved for each catalyst (13842-fold for  $\text{Cu}_2\text{L}_2^1$ , 12054-fold for  $\text{Cu}_2\text{L}_2^2$ , 11934-fold for  $\text{Cu}_2\text{L}_2^3$ ) in the CTAB micellar solution in comparison with the auto-hydrolysis of PNPP at pH 7.0, 25°C. Also, for the complex-promoted PNPP hydrolysis the introducing of CTAB micelles led to 2~3 times acceleration in contrast



**Scheme 2.** Distinguishable distribution (left) of substrate and catalyst in two media, e.g., buffered aqueous solution and CTAB micellar solution. Right illustration shows the micellar catalysis hydrolysis of PNPP by the as-prepared complexes.

with buffered aqueous medium. The CTAB-promoted hydrolysis of PNPP in the absence of binuclear copper(II) complex only gives a small  $k_{\text{ob}}$  value of  $9.0 \times 10^{-5} \text{ s}^{-1}$  showing undesired rate enhancement (about 11.5-fold) as compared to PNPP spontaneous hydrolysis. Table S-5 lists relative activities of PNPP hydrolysis between various catalytic systems each other, indicating that these three copper(II) complexes indeed provide dominative contribution to the rate enhancement of PNPP hydrolysis in contrast with sole CTAB micelles. Obvious acceleration probably results from three major factors<sup>32</sup> (see Scheme 2) deriving from the intrinsic structural property of CTAB micelles. First, reactive molecules including hydrophobic PNPP and complexes are facily solubilized in the micelle phase of CTAB, leading to a higher local concentration of reactants<sup>33</sup> in CTAB micelle phase relative to the lower one in aqueous phase. Second, positive head groups of CTAB micelles provide additional stability of negative tetrahedron transition state.<sup>34</sup> Owing to higher local  $\text{OH}^-$  concentration in the positive head groups region of CTAB micelles, finally, the Cu(II)-bound water undergoes an easier deprotonation to produce nucleophilic hydroxide species compared to bulk phase. This experimental phenomenon is in accordance with those previous reports concerning the increased local basicity due to electrostatic attraction of positive head groups of cationic micelles.<sup>33, 35</sup>

## Conclusions

In our work, three novel binuclear copper(II) complexes with reduced L-serine Schiff bases possess interesting crystal forms, and exhibit better reactivity towards the hydrolysis of p-nitrophenyl acetate (PNPA). Moreover, contrast test was performed for evaluating activities of these complexes in the hydrolysis of another analogue, PNPP (p-nitrophenyl picolinate). The observations shown that PNPP hydrolysis is much faster than the hydrolysis of PNPA, which is attributed to more beneficial intramolecular nucleophilic mechanism of PNPP hydrolysis under comparable conditions. The introducing of CTAB micelles exhibited positive effect on the PNPP hydrolysis in the presence of the as-prepared complexes, announcing 2~3 folds rate enhancement as compared to that in buffered aqueous solution.

## Experimental

### Chemicals and Instruments

All of reagents were analytical grade and used without further purification. Potassium chloride as buffered reagent was purchased from Sigma-Aldrich Co. Tris-H<sup>+</sup> [tris(hydroxymethyl) aminomethane] was purchased from Chengdu Kelong Chemical Co. Surfactant CTAB and three kinds of 5-substituted salicylaldehydes were products of Beijing J&K Scientific Ltd. The reduced L-serine Schiff bases as desired ligands and their respective binuclear copper(II) complex were synthesized by the method described below. Purified water with high resistance of 18 MΩ, which is from a Water Purification System (Nex Power 1000, Human Corporation, South Korea), was used throughout for kinetic determinations. PNPA as aim substrate was provided by our lab, and PNPP as contrast substrate was prepared using previous route.<sup>25</sup> Stock solutions of PNPA and PNPP (C<sub>stock</sub>=0.02 M) were freshly prepared with anhydrous acetonitrile. Hydrolysis rates of PNPA or PNPP was determined by monitoring the changing concentration of p-nitrophenolate anion as detectable product at 400nm on a GBC Cintra 1010 UV-vis spectrometer (Australia GBC Scientific Equipment Pty Ltd).

The <sup>1</sup>H NMR spectrum was recorded at 600 MHz on a Bruker Avance-600 NMR spectrometer (Bruker Corporation, Germany). Mass spectra of the three complexes were recorded on AGILENT 1100 LC-MS (Agilent, USA). Elemental analysis was carried out on CHNOS Elemental Analyzer Vario EL Cube (Germany Elementar Co.). Melting point determination was conducted on X-5-type Digital Precision Melting Point Apparatus (Beijing Fukai Instrument Co., Ltd., China). Single Crystal X-ray Diffraction was recorded with Bruker Smart-Apex-II X-Ray Single-Crystal Diffractometer (Bruker Corporation, Germany). Differential scanning calorimetry (DSC) was determined with DSC200F3 (Netzsch, Germany). Thermal analysis (TG-DTG) was investigated with Netzsch STA409 PC thermal analyzer (Netzsch, Germany). ESI-MS was carried out using Shimadzu LCMS-IT-TOF (Shimadzu Co., Kyoto, Japan).

**General synthesis of reduced L-serine Schiff bases (HL).** L-serine (7mmol) and sodium hydroxide (7mmol) dissolved in 20mL of methanol with stirring, gaining colourless and transparent solution. Then, methanol solution of 5-substituted salicylaldehyde (7mmol) was dropwise added into methanol solution of L-serine. The reaction was further maintained for 3 hours under room temperature. The temperature of yellow reaction residue was controlled at 0-4°C following by the adding of sodium borohydride (NaBH<sub>4</sub>, 7mmol) as reductant. The obtained colourless and transparent solution was adjusted to approximate pH 5.0-6.0 with glacial acetic acid, gradually producing amounts of white precipitates. White precipitates were washed with anhydrous diethyl ether and deionized water for three times during filtration under reduced pressure. Crude precipitates were recrystallized with a mixed solvent of anhydrous methanol and water. Collected white crystals were dried under vacuum at 70°C, generating desired reduced L-serine Schiff bases as aim products. **HL<sup>1</sup>** (containing 5-methyl one): white crystal. Yield 80.6%. m. p. 193-195°C. <sup>1</sup>H NMR (600MHz, DMSO): δ7.05 (1H), 6.99 (1H), 6.75 (1H), 4.02 (2H), 3.79 (1H), 3.65 (1H), 3.24 (1H), 2.19 (3H). **HL<sup>2</sup>** (containing 5-chloro one): white crystal. Yield 89.2%. m. p. 202.4-204.0°C. <sup>1</sup>H NMR (600 MHz, DMSO-d<sub>6</sub>): δ7.32 (1H), 7.19 (1H), 6.84 (1H), 3.97 (2H), 3.75 (1H), 3.64 (1H), 3.25 (1H). **HL<sup>3</sup>** (containing 5-bromo one): white crystal. Yield 78.5%. m.p.195-197°C. <sup>1</sup>H NMR (600 MHz, DMSO-

d<sub>6</sub>): δ7.45 (1H), 7.31 (1H), 6.80 (1H), 3.98-3.96 (2H), 3.76 (1H), 3.65 (1H), 3.25 (1H). DOI: 10.1039/D0DT01823F

**Synthesis and single crystals of binuclear copper(II) complexes with reduced L-serine Schiff bases.** **Cu<sub>2</sub>L<sup>1</sup><sub>2</sub>**: 0.5mmol of HL<sup>1</sup> was dissolved with super-pure water under boiling condition, and then an aqueous solution of 0.6 mmol Cu(OAc)<sub>2</sub>·H<sub>2</sub>O was dropwise added into the solution of HL<sup>1</sup>. Dark green transparent solution was obtained after refluxing for 1h. The dark green filtrate was obtained and cooled to room temperature. Dark green solids were collected for acting as catalyst. To determine absolute structure of this complex, dark green single crystal of Cu<sub>2</sub>L<sup>1</sup><sub>2</sub> suitable for X-ray diffraction was successfully obtained by natural diffusion method. Yield of 78.95%. m. p. >450.0 °C (partial decomposition with about 46.65% residual mass). m/z: calc. for C<sub>22</sub>H<sub>26</sub>Cu<sub>2</sub>N<sub>2</sub>O<sub>9</sub> 589.53; found 590.54 (M+H)<sup>+</sup>, 602. 53 (M+Na)<sup>+</sup>. Anal. calcd. For C<sub>22</sub>H<sub>26</sub>Cu<sub>2</sub>N<sub>2</sub>O<sub>9</sub>: C 44.82, H 4.45, N 4.75; found C 44.81, H 4.46, N 4.74%. Similar preparation was adopted for green Cu<sub>2</sub>L<sup>2</sup><sub>2</sub> and Cu<sub>2</sub>L<sup>3</sup><sub>2</sub>, and their single crystals were also collected for X-ray diffraction determination. **Cu<sub>2</sub>L<sup>2</sup><sub>2</sub>**: yield 82.66%. m. p.>450.0 °C (partial decomposition with about approximate 51.62% residual mass). m/z: calc. for C<sub>20</sub>H<sub>24</sub>Cl<sub>2</sub>Cu<sub>2</sub>N<sub>2</sub>O<sub>10</sub> 650.41; found 651.41 (M+H)<sup>+</sup>, 673.42 (M+Na)<sup>+</sup>. Anal. calcd. For C<sub>20</sub>H<sub>24</sub>Cl<sub>2</sub>Cu<sub>2</sub>N<sub>2</sub>O<sub>10</sub>: C 36.93, H 3.72, N 4.31; found C 36.95, H 3.73, N 4.29%. **Cu<sub>2</sub>L<sup>3</sup><sub>2</sub>**: yield 88.12%. m. p. >450.0 °C (partial decomposition with about 60.14% residual mass). m/z: calc. for C<sub>20</sub>H<sub>20</sub>Br<sub>2</sub>Cu<sub>2</sub>N<sub>2</sub>O<sub>10</sub> 735.28; found 736.29 (M+H)<sup>+</sup>, 778.28 (M+Na)<sup>+</sup>. Anal. calcd. For C<sub>20</sub>H<sub>20</sub>Br<sub>2</sub>Cu<sub>2</sub>N<sub>2</sub>O<sub>10</sub>: C 32.67, H 2.74, N 3.81; found C 32.66, H 2.76, N 3.80%.

### Hydrolysis Kinetics

Kinetics of p-nitrophenyl acetate (PNPA) hydrolysis promoted by the as-resulting binuclear copper(II) complexes were carried out in a pH range of 7.00-8.50 under room temperature. The glass vials containing solution of the buffer, metal complex was thermally equilibrated in a thermostatic compartment. Hydrolysis of PNPA was performed by injecting the PNPA stock solution (an initial concentration of 2.0×10<sup>-2</sup> mol L<sup>-1</sup>) into a 3mL buffer system containing the complex of desired concentration. PNPA concentration was added at least 20 folds excess over the catalyst, resulting in pseudo-first-order kinetics. Pseudo first-order rate constants (k<sub>ob</sub>) were determined by monitoring the appearance of p-nitrophenolate anions (NP) as one product at 400nm. For the aim of comparing substrate selectivity, in addition, this work carried out a control experiment about the catalytic hydrolysis of another substrate (PNPP) promoted by the as-prepared complexes at comparable conditions. Micellar effect of CTAB on the complex-induced PNPP hydrolysis was evaluated under CTAB concentration over its critical micelle concentration (CMC=9.2×10<sup>-4</sup> mol L<sup>-1</sup>). Control run for the PNPP hydrolysis only by CTAB micelles was also performed. All of data reported here are averages of two or three runs with uncertainty of less than 5%.

### Conflicts of Interest

There are no conflicts to declare.

## Acknowledgements

This work was supported by National Natural Science Foundation of China (No. 21771129), Postgraduate Research Project of Chongqing University of Arts and Sciences (No. M2019 ME09). Authors highly appreciate Dr. Qianli Li for analyzing crystal structures. The Sichuan University of Science & Engineering High Performance Computing Center is acknowledged for providing computational.

## Notes and references

[1] (1) B. F. Yan, Carboxylesterases: Part II. Enzyme Systems Involved in Drug Metabolism and Interactions in Animals and Humans. Encyclopedia of Drug Metabolism and Interactions, Ed. by Alexander V. Lyubimov, 2011; (2) D. D. Wang, L. W. Zou, Q. Jin, J. Hou, G. B. Ge and L. Yang, *Acta Pharm. Sin. B*, 2018, **8**, 699-712.

[2] F. Tanaka, *Chem. Rev.*, 2002, **102**, 4885-4906.

[3] J. C. Lugo-González, P. Gómez-Tagle, M. Flores-Alamo and A. K. Yatsimirsky, *Dalton Trans.*, 2020, **49**, 2452-2467; (2) C. Piovezan, R. Jovito, A. J. Bortoluzzi, H. Terenzi, F. L. Fischer, P. C. Severino, C. T. Pich, G. G. Azzolini, R. A. Peralta, L. M. Rossi and A. Neves, *Inorg. Chem.*, 2010, **49**, 2580-2582; (3) T. P. Camargo, A. Neves, R. A. Peralta, C. Chaves, E. C. P. Maia, E. H. Lizarazo-Jaimes, D. A. Gomes, T. Bortolotto, D. R. Norberto, H. Terenzi, D. L. Tierney and G. Schenk, *Inorg. Chem.*, 2018, **57**, 187-203.

[4] S. Rajković, B. Đ. Glišić, M. D. Živković and M. I. Djuran, *Bioorg. Chem.*, 2009, **37**, 173-179.

[5] Z. K. Khoramdareh, S. A. Hosseini-Yazdi, B. Spingler and A. A. Khandar, *Inorg. Chim. Acta*, 2014, **415**, 7-13.

[6] (1) G. Roelfes, *Acc. Chem. Res.*, 2019, **52**, 545-556; (2) F. Schwizer, Y. Okamoto, T. Heinisch, Y. F. Gu, M. M. Pellizzoni, V. Lebrun, R. Reuter, V. Köhler, J. C. Lewis and T. R. Ward, *Chem. Rev.*, 2018, **118**, 142-231.

[7] (1) C. Pan, J. Y. Tang, Y. F. Xu, P. Xiao, H. D. Liu, H. A. Wang, W. B. Wang, F. G. Meng, X. Yu and J. P. Sun, *Sci. Rep. -UK*, 2015, **5**, Article 8560; (2) G. Schenk, N. Mitić, L. R. Gahan, D. L. Ollis, R. P. McGearry and L. W. Guddat, *Acc. Chem. Res.*, 2012, **45**, 1593-1603.

[8] (1) N. H. Williams, B. Takasaki, M. Wall and J. Chin, *Acc. Chem. Res.*, 1999, **32**, 485-493; (2) M. R. Stahley and S. A. Strobel, *Science*, 2005, **309**, 1587-1590.

[9] (1) M. D. Arifuzzaman and Y. Zhao, *ACS Catal.*, 2018, **8**, 8154-8161; (2) S. A. Li, J. Xia, D. X. Yang, Y. Xu, D. F. Li, M. F. Wu and W. X. Tang, *Inorg. Chem.*, 2002, **41**, 1807-1815; (3) B. Xu, W. D. Jiang, F. A. Liu, Y. D. Yu and J. Dong, *Int. J. Chem. Kinet.*, 2015, **47**, 191-198.

[10] (1) H. F. G. Barbosa, M. Attjioui, A. P. G. Ferreira, B. M. Moerschbacher and É. T. G. Cavalheiro, *Int. J. Biol. Macromol.*, 2020, **145**, 417-428; (2) S. Zehra, M. S. Khan, I. Ahmad and F. Arjmand, *J. Biomol. Struct. Dyn.*, 2019, **37**, 1863-1879; (3) M. L. Low, L. Maigre, P. Dorlet, R. Guillot, J.-M. Pagès, K. A. Crouse, C. Policar and N. Delsuc, *Bioconj. Chem.*, 2014, **25**, 2269-2284.

[11] (1) J. Zhang, L. L. Xu and W.-Y. Wong, *Coord. Chem. Rev.*, 2018, **355**, 180-198; (2) A. Trujillo, M. Fuentealba, D. Carrillo, C. Manzur, I. Ledoux-Rak, J. -R. Hamon and J.-Y. Saillard, *Inorg. Chem.*, 2010, **49**, 2750-2764; (3) A. Ionescu, R. Lento, T. F. Mastropietro, I. Aiello, R.

Termine, A. Golemme, M. Ghedini, N. Bellec, E. Pini, I. Rimoldi and N. Godbert, *ACS Appl. Mater. Interf.*, 2015, **7**, 4019-4028. DOI: 10.1021/acsami.5b01823

[12] (1) P. Mahapatra, S. Ghosh, S. Giri, V. Rane, R. Kadam, M. G. B. Drew and A. Ghosh, *Inorg. Chem.*, 2017, **56**, 5105-5121; (2) B. Xu, W. D. Jiang, X. Q. Liu, F. A. Liu and Z. Xiang, *J. Biol. Inorg. Chem.*, 2017, **22**, 625-635; (3) S. P. Tang, P. Hu, H. Y. Chen, S. Chen, Z. W. Mao and L. N. Ji, *J. Mol. Catal. A: Chem.*, 2011, **335**, 222-227.

[13] (1) Z. Asadi and N. Nasrollahi, *J. Mol. Struct.*, 2017, **1147**, 582-593; (2) C. E. Satheesha, P. Raghavendra Kumara, N. Shivakumarb, K. Lingarajuc, P. Murali Krishnab, H. Rajanaikac and A. Hosamani, *Inorg. Chim. Acta*, 2019, **495**, 118929; (3) X. Liu and J. -R. Hamon. *Coord. Chem. Rev.*, 2019, **389**, 94-118; (4) M. Sheoran, K. Bhar, T. A. Khan, A. K. Sharma and S. G. Naik. *Polyhedron*, 2017, **129**, 82-91.

[14] M. A. Neelakantan, F. Rusalraj, J. Dharmaraja, S. Johnsonraja, T. Jeyakumar and M. S. Pillai, *Spectrochim. Acta Part A*, 2008, **71**, 1599-1609.

[15] (1) F. Sevgi, U. Bagkesici, A. N. Kursunlu and E. Guler, *J. Mol. Struct.*, 2018, **1154**, 256-260; (2) S. Zehra, T. Roisnel and F. Arjmand, *ACS Omega*, 2019, **4**, 7691-7705; (3) Ö. Özdemir (nee Güngör), P. Gürkan, B. Özçelik and Ö. Oyardı, *J. Mol. Struct.*, 2016, **1106**, 181-191.

[16] (1) D. E. Koshland Jr, *PNAS*, 1958, **44**, 98-114; (2) D. E. Koshland Jr, *Angrew Chem. Int. Ed. Engl.*, 1994, **33**, 2375-2378; (3) D. E. Koshland Jr., *FEBS Lett.*, 1976, **62(S1)**, E47-E52.

[17] (1) Q. Z. Yao, M. Tian and C. L. Tsou, *Biochemistry*, 1984, **23**, 2740-2744; (2) C. L. Tsou, *Science*, 1993, **262**, 380-381; (3) C L Tsou, *Trends Biochem. Sci.*, 1986, **11**, 427-429.

[18] (1) R. S. Alexander, S. K. Nair and D. W. Christianson, *Biochemistry*, 1991, **30**, 11064-11072; (2) M. Zürcher and F. Diederich, *J. Org. Chem.*, 2008, **73**, 4345-4361; (3) K.-H. Kim, R. Song and K. M. Kim. *J. Am. Chem. Soc.*, 2003, **125**, 7170-7171.

[19] (1) A. Polyzos, A. B. Hughes and J. R. Christie, *Langmuir*, 2007, **23**, 1872-1879; (2) E. Kimura, H. Hashimoto and T. Koike, *J. Am. Chem. Soc.*, 1996, **118**, 10963-10970; (3) C. Schattschneider, S. D. Kettenmann, S. Hinojosa, J. Heinrich and N. Kulak. *Coord. Chem. Rev.*, 2019, **385**, 191-207.

[20] (1) A. P. Gerola, E. H. Wanderlind, Y. S. Gomes, L. A. Giusti, L. García-Río, R. A. Nome, A. J. Kirby, H. D. Fiedler and F. Nome, *ACS Catal.*, 2017, **7**, 2230-2239; (2) P. Scrimin, P. Tecilla and U. Tonellato, *J. Org. Chem.*, 1991, **56**, 161-166; (3) F. Hampl, F. Liska, F. Mancin, P. Tecilla and U. Tonellato, *Langmuir*, 1999, **15**, 405-412; (4) W. D. Jiang, B. Xu, Q. Lin, J. Z. Li, H. Y. Fu, X. C. Zeng and H. Chen. *Colloid Surface A*, 2008, **315**, 103-109; (5) W. D. Jiang, B. Xu, Q. Lin, J. Z. Li, F. A. Liu, X. C. Zeng, H. Chen, *J. Colloid Interf. Sci.*, 2007, **311**, 530-536.; (6) M. F. Torres, R. H. de Rossi and M. A. Fernández, *RSC Adv.*, 2014, **54**, 28606-28614.

[21] A. W. Addison, T. N. Rao, J. Reedijk, J. van Rijn and G. C. Verschoor, *J. Chem. Soc. Dalton Trans.*, 1984, 1349-1356.

[22] S. Albedyhl, D. Schnieders, A. Jancsó, T. Gajda and B. Krebs, *Eur. J. Inorg. Chem.*, 2002, **2002**, 1400-1409.

[23] X. Q. Liu, X. He, N. X. Qiu, X. Yang, Z. Y. Tian, M. J. Li and Y. Xue, *Appl. Surf. Sci.*, 2016, **389**, 894-905.

[24] J. Suh, M. Cheong and H. Han, *Bioorg. Chem.*, 1984, **12**, 188-196.

## ARTICLE

## Journal Name

[25] D. S. Sigman and C. T. Jorgensen, *J. Am. Chem. Soc.*, 1972, **94**, 1724-1730.

[26] (1) K. Yang, E. Strauss, C. Huerta and H. Zhang, *Biochemistry*, 2008, **47**, 1369-1380; (2) Y. Snitko, S. K. Han, B. I. Lee and W. Cho, *Biochemistry*, 1999, **38**, 7803-7810; (3) A. G. Hamre, E. E. Frøberg, V. G. H. Eijsink and M. Sørli. *Arch. Biochem. Biophys.*, 2017, **620**, 35-42.

[27] (1) E. Kuatsjah, A. C. K. Chan, T. E. Hurst, V. Snieckus, M. E. P. Murphy and L. D. Eltis, *ACS Catal.*, 2018, **8**, 11622-11632; (2) R. S. Heying, M. P. da Silva, G. S. Wecker, R. A. Peralta, A. J. Bortoluzzi and A. Neves, *Inorg. Chem. Commun.*, 2019, **102**, 245-250.

[28] (1) B. Y. Jiang, Y. Xiang, J. Du, J. Q. Xie, C. W. Hu, X. G. Zeng. *Colloids Surfaces A.*, 2004, **235**, 145-151; (2) J. Q. Xie, S. Q. Cheng, B. Y. Jiang, J. Du, C. W. Hu, X. G. Zeng. *Colloids Surfaces A.*, 2004, **235**, 137-143.

[29] N. Mitić, S. J. Smith, A. Neves, L. W. Guddat, L. R. Gahan and G. Schenk, *Chem. Rev.*, 2006, **106**, 3338-3363; (2) M. A. Wells and T. C. Bruice, *J. Am. Chem. Soc.*, 1977, **99**, 5341-5356; (3) F. G. Maranhã, G. A. dos S. Silva, A. J. Bortoluzzi, E. Nordlander, R. A. Peralta and A. Neves, *Inorg. Chim. Acta*, 2020, **502**, article 119280; (4) A. G. Blackman and L. R. Gahan, *ZAAC*, 2018, **644**, 16-629.

[30] P. W. Chang, A. Madabushi and A. L. Lu, *BMC Biochem.*, 2009, **10**, 19.

[31] S. C. Graham, P. E. Lilley, M. Lee, P.M. Schaeffer, A. V. Kralicek, N. E. Dixon and J. M. Guss, *Biochemistry*, 2006, **45**, 964-975.

[32] S. Bhattacharya and N. Kumari, *Coord. Chem. Rev.*, 2009, **253**, 2133-2149.

[33] (1) F. M. Menger, L. H. Gan, E. Johnson and D. H. Durst, *J. Am. Chem. Soc.*, 1987, **109**, 2800-2803; (2) B. Xu, W. D. Jiang, Y. Wang, Z. Xiang, F. A. Liu and Y. Wu, *Colloid Surface A*, 2014, **456**, 222-230.

[34] (1) M. N. Al-Shamary, H. A. Al-Lohedan, M. Z. A. Rafiquee, F. El-Ablack and Z. A. Issa, *J. Saudi Chem. Soc.*, 2017, **21**, Supplement 1, s193-s201; (2) I. Brandariz and E. Iglesias, *Colloid Surface A*, 2014, **454**, 180-188.

[35] (1) Y. Sarkar, S. Das, A. Ray, S. K. Jewrajka, S. Hirota and P. P. Parui, *Analyst*, 2016, **141**, 2030-2039; (2) S. Bhattacharya and V. P. Kumar, *Langmuir*, 2005, **21**, 71-78.

View Article Online  
DOI: 10.1039/D0DT01823F

## Table of Contents

## Structures and Esterolytic Reactivity of Novel Binuclear Copper(II) Complexes with Reduced L-Serine Schiff Bases as Mimic Carboxylesterases

Qin Zhang,<sup>a</sup> Jun Shu,<sup>a</sup> Yajun Zhang,<sup>b</sup> Zhigang Xu,<sup>b</sup> Jian Yue,<sup>a</sup> Xiaoqiang Liu<sup>a\*\*</sup>, Bin Xu,<sup>a</sup> Zhongzhu Chen<sup>b</sup>  
and Weidong Jiang<sup>a\*</sup>

Three novel binuclear copper(II) complexes with reduced L-serine Schiff bases exhibited significant activity difference for the hydrolysis of PNPA and PNPP, suggesting favourable intramolecular nucleophilic pathway for PNPP. The introducing of CTAB micelles arouses 2.0 ~ 3.2 folds rate enhancement for PNPP hydrolysis against buffered aqueous solution.

